Estimation of the shear force in transverse dynamic force microscopy using a sliding mode observer

Thang Nguyen,[1] Toshiaki Hatano,[2] Said G Khan,[2] Kaiqiang Zhang,[2] Christopher Edwards,[1] Robert Harniman,[3] Stuart C. Burgess,[2] Massimo Antognozzi,[3] Mervyn Miles,[3] and Guido Herrmann[2, a)]

[1)]*College of Engineering, Mathematics & Physical Sciences, University of Exeter, Exeter, EX44QF, UK*

[2)]*Department of Mechanical Engineering, University of Bristol, Bristol, BS81TR, UK*

[3)]*Centre for Nanoscience & Quantum Information, University of Bristol, Bristol, BS81FD, UK*

In this paper, the problem of estimating the shear force affecting the tip of the cantilever in a *Transverse Dynamic Force Microscope* (TDFM) using a real-time implementable sliding mode observer is addressed. The behaviour of a vertically oriented oscillated cantilever, in close proximity to a specimen surface, facilitates the imaging of the specimen at nanometre scale. Distance changes between the cantilever tip and the specimen can be inferred from the oscillation amplitudes, but also from the shear force acting at the tip. Thus, the problem of accurately estimating the shear force is of significance when specimen images and mechanical properties need to be obtained at submolecular precision. A low order dynamic model of the cantilever is derived using the method of lines, for the purpose of estimating the shear force. Based on this model, an estimator using sliding mode techniques is presented to reconstruct the unknown shear force, from only tip position measurements and knowledge of the excitation signal applied to the top of the cantilever. Comparisons to methods assuming a quasi-static harmonic balance are made.

[a)]Corresponding Author: G.Herrmann@bris.ac.uk

Atomic Force Microscopy (AFM) has become a widespread and important technique for the study of nano-scale specimens since its inception in 1986 by Binnig *et al.*[1]. Broadly speaking, an AFM can provide high resolution images in different settings including ambient, aqueous and vacuum environments. This makes it especially suitable for the investigation of biological specimens under physiological conditions. A key component in most AFMs is a micro-cantilever. The interaction between the tip of the cantilever and the sample creates bending/shear moments on the cantilever, which can be indirectly measured via a laser based sensor system. This is then used to create a high resolution topographical image via a raster scan over the specimen surface. In standard AFMs, the cantilever is mounted horizontally and the devices are operated in a contact[1] or intermittent-contact mode[2,3]. In contrast, the *Transverse Dynamic Force Microscope* (TDFM) at Bristol addresses the problem of non-contact imaging of a sample. This is important for certain types of biological specimens. Under ambient room conditions, any sample will be covered by an ordered, thin water layer; hence, recorded changes in the cantilever resonant dynamics measure the short-range lateral forces between an oscillating vertically oriented cantilever (VOC) and a surface. It has been demonstrated that the visco-elastic response of the ordered water layer between the tip and the surface results in a contrast mechanism[4–7] for cantilever-specimen distance detection. The "snap-to-contact" behaviour is experienced by conventional AFMs. This is due to the gradient of the surface attractive force being larger than the spring constant of the cantilever[8]. In the TDFM, this is prevented by the vertical orientation of the cantilever.

Because of the pivotal role of the micro-cantilever, it is important to understand its dynamic behaviour and to have knowledge of its physical parameters and characteristics. Unsurprisingly, the problem of estimating the cantilever parameters in AFM devices has been investigated for many years in the literature. A real-time methodology to determine the probe loss areas in a dynamic atomic force microscopy based image was established by De *et al.*[9] and an observer-based approach for estimating some unknown force affecting the dynamics of a cantilever in *Electric Force Microscopy* devices was proposed by Besancon *et al.*[10]. More recently, the tip-sample interaction forces based on a two degree of freedom mathematical model of a tapping mode AFM was investigated by Xu *et al.* when the cantilever is immersed in liquid[11]. However, all these results pertain to horizontally mounted cantilever arrangements.

This paper addresses the problem of estimating the tip-sample interaction forces with a real-time implementable sliding mode observer[12–15] for the TDFM, which operates in a non-contact scanning regime with a vertically oriented cantilever. Sliding mode observers have the advantage of

robustly detecting unknown signals with finite time convergence guarantees[13]. Comparisons with a quasi-static method (as often employed in beam analysis) are made. This approach is realized under additional assumptions which are not required for the sliding mode observer.

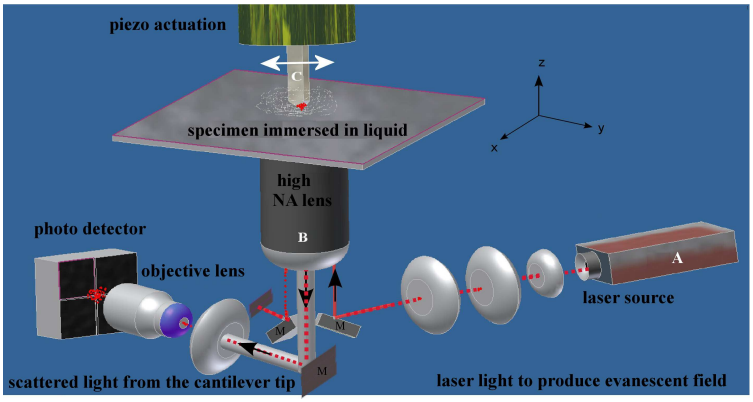

FIG. 1. Simplified schematic of the TDFM together with a scattered evanescent wave (SEW) system (adopted from Harniman *et al.*[16], © [2015] IEEE. Reprinted, with permission, from T. Nguyen, S. G. Khan, C. Edwards, G. Herrmann, L. Picco, R. Harniman, S. C. Burgess, M. Antognozzi, and M. Miles "Estimation of the shear force in transverse dynamic force microscopy using a sliding mode observer", in *American Control Conference, 2013* (2013) pp. 5514 – 5519.)

A schematic of the TDFM setup is shown in Figure 1. In the TDFM, the scattered evanescent field from the cantilever tip is gathered by a lens (B) with large numerical aperture (NA) and transmitted to the objective lens. The objective lens then focuses the light onto the photo-diode. The amplitude variations (both in x and y directions) and the height (z) of the cantilever tip relative to the cover slip can be measured via the signals coming from the four sectors of the photo-diode. (In reality the actual TDFM system is more complex and detailed than the schematic presented in Figure 1, which only shows the main components.[16]) The available data for the estimation (and control) problems are the excitation signal at the top of the cantilever, the distance (z) of the cantilever from the cover slip (the summed light intensity of all photo diode sectors) and the horizontal position of the cantilever tip (obtained from suitably scaled light-intensity signals from the photo-diode sectors).

Since the cantilever specimen distance cannot be directly measured, other factors should be taken into account to construct the specimen topography. Hence, understanding the behaviour of the shear forces helps to improve the mechanism for detecting the probe/specimen distance.

The dynamics of the cantilever in air, with the shear force interaction due to a thin water layer at

the tip, can be presented in the form of the partial differential equation (PDE)[18,19]

$$\frac{\partial^4 EI(Y+\alpha\dot{Y})}{\partial\zeta^4}+\rho S\ddot{Y}=0 \tag{1}$$

with boundary conditions

$$Y(\zeta=0)=u(t), \tag{2}$$

$$\frac{\partial Y}{\partial\zeta}(\zeta=0)=0, \tag{3}$$

$$\frac{\partial^2 Y}{\partial\zeta^2}(\zeta=L)=0, \tag{4}$$

$$EI\frac{\partial^3 Y}{\partial\zeta^3}(\zeta=L)=-f(t), \tag{5}$$

In the above, E is Young's modulus, α is the internal damping constant of the cantilever, I is the secondary moment of area, S is the cross-sectional area, ρ is the density of the probe, L is the length of the cantilever, ζ denotes position along the probe axis, Y is the transversal displacement at any point along the probe during vibration, $\dot{Y}$ and $\ddot{Y}$ are the first and second derivatives of Y with respect to time t, $u(t)$ is the external excitation signal applied at the top of the cantilever, and finally $f(t)$ is the tip-sample interaction force applied at the tip of the cantilever. The aim of this paper is to estimate the unknown shear force signal $f(t)$, which will allow better interpretation and understanding of the scan result.

The infinite dimensional PDE in (1) is not convenient for real-time implementation and for the estimation methods to be applied[12–15]. Given the measured tip position $Y(\zeta=L)$, the shear force $f(t)$ and the excitation signal $u(t)$, it is necessary to approximate the dynamic relationship between those three variables via a finite dimensional ordinary differential equation (ODE). This is achieved by the method of lines[20]. The idea is to divide the cantilever probe into $n-1$ equal sections and to consider n nodes distributed along the probe. Denote Y_j as the displacement at node j and $\delta\zeta$ as the distance between two consecutive nodes. Using a finite difference formula the boundary condition (3) for the approximate model becomes

$$\frac{\partial Y}{\partial\zeta}(\zeta=0)\approx\frac{Y_2-Y_1}{\delta\zeta}=0 \quad \Rightarrow Y_2=Y_1. \tag{6}$$

Thus, for the boundary condition (4), the relation is obtained

$$Y_n-2Y_{n-1}+Y_{n-2}=0. \tag{7}$$

The right hand side of (5) can be approximated as

$$EI\frac{\partial^3 Y}{\partial \zeta^3}(\zeta = L) \approx EI_n \frac{Y_n - 3Y_{n-1} + 3Y_{n-2} - Y_{n-3}}{\delta\zeta^3}. \tag{8}$$

Equations (2), (6), (7) and (8) imply that the values of Y_1, Y_2, Y_n, and Y_{n-1} are 'known', i.e. depend on the dynamics of the remaining nodes. Hence, understanding the dynamics of the remaining 'middle' $n-4$ nodes is key. From (1), the fourth partial derivative of Y with respect to the spatial variable ζ can be approximated using finite differences as follows

$$\frac{\partial^4 Y_j}{\partial \zeta^4} \approx \frac{Y_{j+2} - 4Y_{j+1} + 6Y_j - 4Y_{j-1} + Y_{j-2}}{\delta\zeta^4} \tag{9}$$

for $j = 3, ..., n-2$. Using the boundary conditions (6), (7) and (8), and the approximate model (9), the dynamics of nodes Y_j for $j = 3, ..., n-2$ are obtained. A linear time invariant system based on the dynamics of Y_j for $j = 3, ..., n-2$ is used. The relations between Y_j, $\dot{Y}_j$, f, and u allow the establishment of an ODE of order $2(n-4)$. Using a matrix-vector representation, this ODE is written as a state-space system[21] with a dynamic state variable vector $x_p(t)$ of dimension $2(n-4)$, in the form

$$\begin{aligned} \dot{x}_p(t) &= A_p x_p(t) + B_p u(t) + D_p f(t) \\ y(t) &= C_p x_p(t) \end{aligned} \tag{10}$$

where the matrices A_p, B_p, D_p, and C_p are of appropriate size. Crucially, (10) is a good approximation of the PDE providing $\delta\zeta$ is small enough. In (10) the output $y(t)$ which represents the cantilever tip position is taken as Y_{n-2} since it is assumed that $Y_n \approx Y_{n-2}$ for large enough n. Furthermore the shear force can be approximated by a linear combination of the state variables x_p in (10) without the knowledge of the derivative of Y_n. Further details can be found in Nguyen *et al.*[17]. Clearly the larger the number of nodes, the more accurately (10) approximates the real PDE (1). However the greater the number of nodes, the higher the order of the state-space and the greater the computational burden. For this reason, a lower order (approximate) model of (10) is more desirable. To create such a model, a broad range of methods for model order reduction, available in the systems theory literature, can be employed: see for example[22,23] and the references therein. Here the 'balanced truncation' method by Moore[22], has been used. Hence, for design purposes, a model of the form

$$\begin{aligned} \dot{x}(t) &= Ax(t) + Bu(t) + Df(t) \\ y(t) &= Cx(t) \end{aligned} \tag{11}$$

is used with the property that the input/ouput behaviour $(u, f) \mapsto y$ of (11) closely matches that of (10). The key property of (11) compared to (10) is that the dimension of the vector $x(t)$ is orders

of magnitude lower than $x_p(t)$. Although the elements of $x(t)$ no longer have physical meaning, this system is now ideal for design of the shear force estimator.

In (11) the inputs $u(t)$ and $y(t)$ are known and measured. However the state, $x(t)$, and in particular the shear force, $f(t)$, are unknown. Here a so-called sliding mode observer (see for example[12–15] and the references therein) will be used to estimate $f(t)$ from the known quantities $y(t)$ and $u(t)$ and knowledge of the model in (11). In this paper, a design proposed in Edwards *et al.*[12] is employed. The sliding mode observer has the following form:

$$\dot{\hat{x}}(t) = A\hat{x}(t) + Bu(t) - Ge_y(t) - Dk\text{sgn}(e_y(t)) \tag{12}$$

$$\hat{y}(t) = C\hat{x}(t) \tag{13}$$

where $k > 0$ is a scalar gain, $\text{sgn}(\cdot)$ represents the signum function and the output estimation error

$$e_y(t) = \hat{y}(t) - y(t) \tag{14}$$

is the difference between the output of the observer $\hat{y}(t)$ and the measured value $y(t)$. The gain G represents design freedom and must be selected to ensure the matrix $(A - GC)$ is Hurwitz stable (i.e. the eigenvalues of the matrix $(A - GC)$ have negative real part, e.g.[14]). It can be shown that for an appropriate choice of G and the scalar gain k, the output estimation error $e_y(t)$ is driven to zero *in finite time* and a so-called sliding motion takes place[12,14]. During the sliding motion, on average, the high frequency switching term $-k\text{sgn}(e_y(t))$ must replicate $f(t)$ for sliding to be maintained. The average value of $k\text{sgn}(e_y(t))$ necessary to maintain sliding is known as the equivalent injection[14,24] and can be approximated by low-pass filtering the actual injection signal $k\text{sign}(e_y(t))$. Here a simple first-order low-pass filter for the fast-switching value of $k\text{sgn}(e_y(t))$ is used to obtain the estimate, $\tilde{f}(t)$, of the shear force from the equivalent injection. Let $\tilde{f}(t)$ satisfy

$$\dot{\tilde{f}}(t) = -\frac{1}{\tau}(\tilde{f}(t) + k\text{sgn}(e_y(t))). \tag{15}$$

where τ is a small positive scalar which represents the filter time constant. Since $\tilde{f}(t)$ approximates the equivalent injection[24], it follows $\tilde{f}(t) \approx f(t)$. Note that $\tilde{f}(t)$ is available in real time from (15) and as a result, changes in the shear force $f(t)$ can be estimated in real time. A diagram of the observer and further explanations are presented in Figure 2.

The experiments which follow were carried out at ambient conditions, which were 20 °C and a room humidity of 60%. The external excitation $u(t) = d_0 \sin(\omega t)$ is sinusoidal with frequency ω

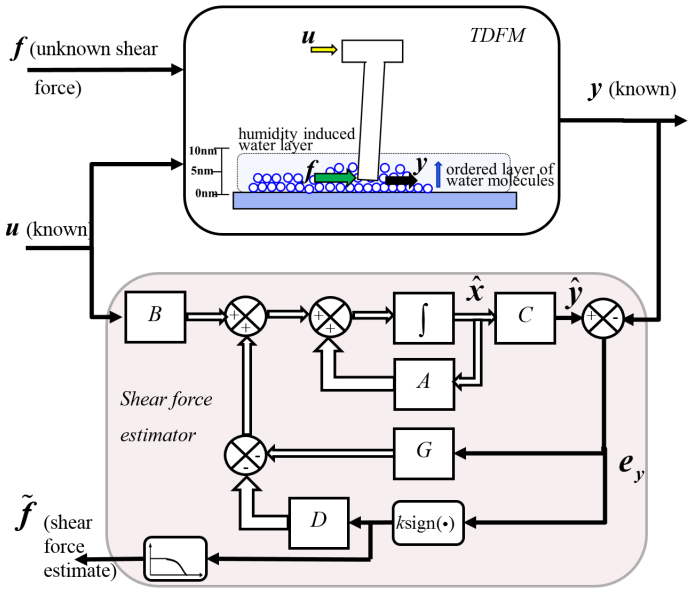

FIG. 2. TDFM and nonlinear sliding mode observer based estimator of the shear force f given an excitation signal $u(t)$ at the top of the cantilever and the measured position $y(t)$ of the tip of the cantilever. The error signal $e_y(t)$ (14) creates the drivers for the estimator, the observer injection term $k\text{sgn}(e_y(t))$ and $Ge_y(t)$, to guarantee fast and robust convergence. The low pass filtering of the switching observer injection $k\text{sgn}(e_y(t))$ provides the shear force estimate $\tilde{f}(t)$

and amplitude d_0. Furthermore, it is assumed that the tip sample interaction force at the tip can be split into a viscous and an elastic force[18]:

$$f(t) = -\nu \frac{\partial Y}{\partial t}(L,t) - \kappa Y(L,t) \tag{16}$$

where ν is the dissipative interaction constant and κ is the elastic interaction constant. The cantilever is made of Silicon Nitride (Si3N4) and the parameters are given as follows: Young's modulus E=210 GPa, ρ=3100 kg/m^3, length L=28 μm, width w=2 μm, thickness t_c=200 nm. The cantilever was brought within a distance of 10 nm to a quartz cover slip (No. 0, i.e. 85-130 μm thick) to initially determine an excitation-to-cantilever model in free air. This yielded the necessary data to obtain a reduced-order state space model (11). Then, fourteen data sets X_1, X_2, X_3,...X_{14}, including input and output signals, were collected from experiments. The tip-to-surface distances corresponding to X_1, X_2, X_3,...X_{14} are linearly increasing for 1.5 nm to 8 nm respectively. The top of the cantilever was excited at its resonance frequency of 352.75 kHz. The amplitude of the excitation signal is 1.8 nm.

Using the model (11), a sliding mode estimator was designed. An example of a shear force es-

timate is shown in Figure 3(a) which exhibits sinusoidal signals with the same frequency as the excitation signal $u(t)$. The inherent bandwidth limit of the sliding mode observer design is given by the low pass filter time constant $\tau = 5\mu s$ from (15). Figure 3(b) provides the RMS values $\tilde{f}_{eff}$ (RMS - root mean square values) of the shear force estimates for each data series. It is clear that the shear forces corresponding to the data sets recorded close to the cover slip exhibit the largest interaction, i.e. the first data sets have the biggest amplitudes among the shear forces. It is now also possible to estimate the elastic and viscous parameters κ and ν (e.g. using a recursive least squares process). This introduces a further time constant of $5\mu s$ associated with the recursive least squares process. This time constant and the filter time constant τ in (15) are independent of a quasi-static harmonic balance assumption and are the result of well-understood linear filtering processes. It was observed that the elastic component $-\kappa Y(L,t)$ contributes less than 1.3 % to the overall shear force energy so that this term can be disregarded. In contrast, the estimates of the viscous coefficient (see Figure 3(c)) follow, within the tip-to-surface range of 2-8 nm, a generally decreasing relation. This confirms the viscous effect of the thin water layer above the cover slip, which increases the closer the cantilever tip is to the cover slip. Note the significant difference in magnitude change for ν and $\tilde{f}_{eff}$. This is due to uncorrelated sensor noise in the output signal $y(t) = Y(L,t)$. Whilst the least squares methods for ν remain largely unaffected by this, the RMS-value $\tilde{f}_{eff}$ is.

An important aspect of the sliding mode observer is its ability to work without the requirement of harmonic excitation and measurement signals, including a steady state assumption of the overall system under this condition. However, the TDFM adheres to these assumptions at least within some quasi-steady state. For comparative reasons, given the sinusoidal characteristics of the excitation $u(t)$ and the cantilever tip position $y(t)$, it is possible to compute the sinusoidal components of $f(t)$, and subsequently the viscous coefficient ν of $f(t)$ (see[18,19] for a generic tapered beam and[25] for a homogenous beam as used here). The derivation of the amplitude and phase for $y(t)$ in relation to $u(t)$ is done via a real-time implementable phase-locked loop (PLL) technique[26]. It is well-known that a phase-locked loop technique has at its *very best* an inherent settling time of one oscillation period (see for example Chapter 3[26]), i.e. $2.83\ \mu s = 1/(352.75kHz)$. However, realistically the pull-in process of a PLL is several multiples of one oscillation period - the direct result of a nonlinear process of the PLL. Thus, for the estimation of the viscous component ν, the PLL relative to the sliding mode technique provides in Figure 4 a delayed result of about 40 μs. Cantilever data for tip-to-surface distances between 1.5 nm to 6.5 nm were used. The PLL-results

for v appear to be 'low-pass-filtered' in relation to the sliding mode estimate, i.e. they are of lower frequency content and delayed. Considering the requirement for high-speed scanning and subsequent high-speed data processing, the sliding mode observer shows an advantage over the PLL-method in terms of speed and the basic underlying technical assumptions.

In conclusion, a constructive scheme to obtain a real time estimate of the shear forces affecting the VOC of a TDFM has been presented. A parametric representation of the shear force presents a scaled measure of the cantilever-specimen distance. An approximate ODE model of the cantilever dynamics was derived using the method of lines[20]. Based on this ODE model, a reduced order model was used to construct a sliding mode observer to estimate the unknown shear force. Practical examples illustrate that the proposed real-time implementable scheme can reconstruct the unknown shear forces using measurement signals subject to noise. The model confirms an increase in viscous damping as the distance between the cantilever and the cover slip decreases. The method shows faster response times and higher bandwidth than a phase-locked loop based technique which operates under the assumption of a quasi-steady state balance of harmonic excitation and output signals.

ACKNOWLEDGMENTS

This research is supported under the EPSRC grants EP/I034882/1 & EP/I034831/1.

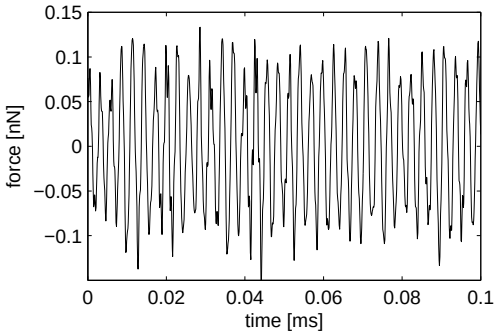

(a)Estimate of shear force for data X_1 for a cantilever/cover slip distance of 1.5 nm

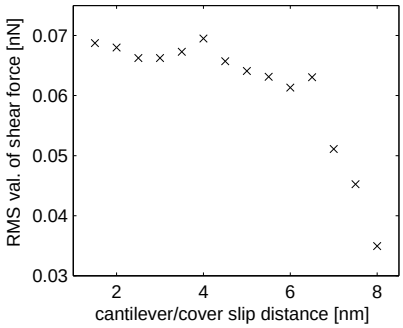

(b)RMS value $\tilde{f}_{eff}$ of shear force $\tilde{f}$ as a function of the cantilever-cover slip distance

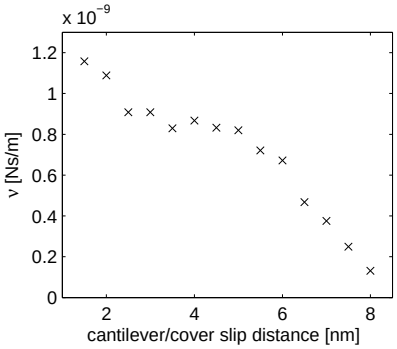

(c)Estimate of viscous coefficient ν as a function of the cantilever-cover slip distance

FIG. 3. Shear force estimate characteristics

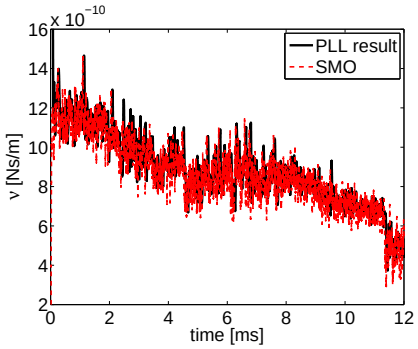

(a)Estimate of shear force for data

varying between 1.5 nm-6.5 nm

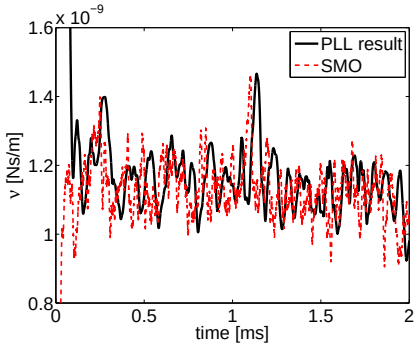

(b)Estimate of shear force for data

varying between 1.5 nm-2 nm

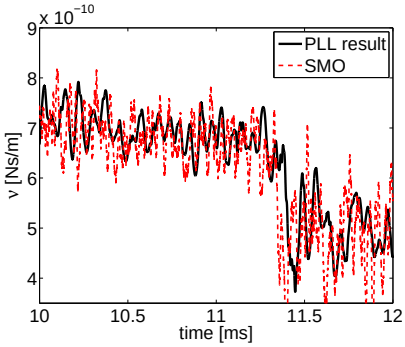

(c)Estimate of shear force for data

varying between 5.5 nm-6.5 nm

FIG. 4. Shear force estimate characteristics as function of time for sliding mode (SMO) and PLL-technique

REFERENCES

[1]G. Binnig, C. Quate, and C. Gerber, "Atomic force microscope," Physical Review Letters (1986).

[2]K. A. Ramirez-Aguilar and K. L. Rowlen, "Tip characterization from AFM images of nanometric spherical particles," Langmuir **14**, 2562–2566 (1998).

[3]R. Howland and L. Benatar, *Practical Guide to Scanning Probe Microscopy* (Park Scientific Instruments: Sunnyvale, CA, USA, 1993).

[4]M. Antognozzi, A. Humphris, and M. Miles, "Observation of molecular layering in a confined water film and study of the layers viscoelastic properties," Applied Physics Letters **78**, 300–302 (2001).

[5]P. J. James, M. Antognozzi, J. Tamayo, T. J. McMaster, J. M. Newton, and M. J. Miles, "Interpretation of contrast in tapping mode AFM and shear force microscopy: a study of Nafion," Langmuir **17**, 349–360 (2001).

[6]R. Brunner, O. Marti, and O. Hollricher, "Influence of environmental conditions on shearforce distance control in near-field optical microscopy," Journal of Applied Physics **86**, 7100–7106 (1999).

[7]S. Davy, M. Spajer, and D. Courjon, "Influence of the water layer on the shear force damping in near-field microscopy," Journal of Applied Physics **73**, 7594–7596 (1998).

[8]N. A. Burnham and R. J. Colton, "Measuring the nanomechanical properties and surface forces of materials using an atomic force microscope," Journal of Vacuum Science Technology (1989).

[9]T. De, P. Agarwal, D. R. Sahoo, and M. V. Salapaka, "Real-time detection of probe loss in atomic force microscopy," Applied Physics Letters **89**, 133119–1–133119–3 (2006).

[10]G. Besancon, A. Voda, and M. Alma, "On observer-based estimation enhancement by parametric amplification in a weak force measurement device," in *CDC 2008. 47th IEEE Conference on Decision and Control, 2008.* (2008) pp. 5200 –5205.

[11]X. Xu, J. Melcher, and A. Raman, "Accurate force spectroscopy in tapping mode atomic force microscopy in liquids," Phys. Rev. B **81**, 035407–1–035407–7 (2010).

[12]C. Edwards and S. K. Spurgeon, "Sliding mode output tracking with application to a multivariable high temperature furnace problem," International Journal of Robust and Nonlinear Control **7**, 337–351 (1997).

[13]C. Edwards, S. K. Spurgeon, and R. J. Patton, "Sliding mode observers for fault detection and

isolation," Automatica **36**, 541 – 553 (2000).

[14]C. Edwards and S. Spurgeon, *Sliding Mode Control: Theory and Applications* (Taylor & Francis, 1998).

[15]C. P. Tan and C. Edwards, "Robust fault reconstruction in uncertain linear systems using multiple sliding mode observers in cascade," IEEE Transactions on Automatic Control **55**, 855 –867 (2010).

[16]R. L. Harniman, J. A. Vicary, J. K. H. Hörber, L. M. Picco, M. J. Miles, and M. Antognozzi, "Methods for imaging DNA in liquid with lateral molecular-force microscopy," Nanotechnology **23**, 085703 (2012).

[17]T. Nguyen, S. G. Khan, C. Edwards, G. Herrmann, L. Picco, R. Harniman, S. C. Burgess, M. Antognozzi, and M. Miles, "Estimation of the shear force in transverse dynamic force microscopy using a sliding mode observer," in *American Control Conference, 2013* (2013) pp. 5514 – 5519.

[18]M. Antognozzi, *Investigation of the shear force contrast mechanism in transverse dynamic force microscopy*, Ph.D. thesis, Univeristy of Bristol (2000).

[19]M. Antognozzi, D. Binger, A. Humphris, P. James, and M. Miles, "Modeling of cylindrically tapered cantilevers for transverse dynamic force microscopy (TDFM)," Ultramicroscopy **86**, 223 – 232 (2001).

[20]W. E. Schiesser and G. W. Griffiths, *A compendium of partial differential equation models: method of lines analysis with Matlab* (Cambridge University Press, 2009).

[21]K. J. Aström and R. M. Murray, *Feedback systems: an introduction for scientists and engineers* (Princeton University Press, 2010).

[22]B. Moore, "Principal component analysis in linear systems: Controllability, observability, and model reduction," IEEE Transactions on Automatic Control **26**, 17 – 32 (1981).

[23]A. C. Antoulas, *Approximation of Large-Scale Dynamical Systems* (Society for Industrial and Applied Mathematics, 2005).

[24]V. Utkin, *Sliding Modes in Control Optimization* (Springer-Verlag, Berlin, 1992).

[25]T. Nguyen, C. Edwards, G. Herrmann, T. Hatano, S. Burgess, and M. Miles, "Cantilever dynamics modelling for the transverse dynamic force microscope," in *2014 IEEE 53rd Annual Conference on Decision and Control (CDC)* (2014) pp. 1318–1323.

[26]R. E. Best, *Phase locked loops - Design, Simulation and Applications* (McGraw-Hill Professional, 2007).